

## CHAPTER III

### RESULTS

#### 3.1 Design of artificial ankyrin repeat motif for library construction

The ultimate goal in library construction is to design the consensus repeat modules which contain the fixed conserve-framework residues and the randomized potential target interaction residues. The consensus proposed in this study was based on the previous constructed library called ‘Designed Ankyrin Repeat Proteins (DARPin) library’ with an advance in the strategy for library generation to comprise the randomization not only in amino acids but also the number of repeats. Moreover, degenerated codons in interacting residues were designed to bias the amino acids distribution at each position toward the distribution observed in databases of natural sequences. The single internal repeat of ankyrin template was subjected to align with the databases. The 3485 and 1180 sequences of natural ankyrin repeats from Prosite (PS50088) and Pfm (PF00023) database were retrieved. Only repeats without extra insertions or deletions were recruited for alignment and subsequently submitted to generate the sequence logo. A sequence logo is a graphical representation of an amino acid multiple sequence alignment. Each logo consists of stacks of symbols, one stack for each position in the sequence. The overall height of the stack indicates the sequence conservation at that position, while the height of symbols within the stack indicates the relative frequency of each amino or nucleic acid at that position.

Sequence logos were generated using weblogo website (WebLogo, <http://weblogo.berkeley.edu/>).

The sequence logo of obtained natural ankyrin repeats was generated as shown in **Figure 3.1A**. The order of amino acid was re-numbered with the respect to DARPin library. The resulting alignment of all sequences yielded the consensus containing highly randomized residues at position 2, 3, 5, 10, 13, 14, 17, and 33. Other positions were defined as framework residues. Second step, the consensus sequence was defined based on DARPins and resulting alignments with some modifications as shown in **Figure 3.1B**. Amino acids at positions 26 and 33 were preserved as histidine (H) and arginine (R), respectively. Glutamic acid (E) and valine (V) at position 21 and 22 were changed to arginine (R) and leucine (L) for inserting *Bsm* BI restriction site. Additionally, lysine (K) at position 25 was substituted with E to prevent the electrostatic problem with R at position 21.

The 3D structure of our consensus with substitutions (1D4\_binder) was generated using Accelrys Discovery Studio version 2.5 software. The minimized structure of 1D4\_binder was superimposed with template (E3\_5 template). As shown in **Figure 3.2**, the structure of generated consensus was not critically changed from the template, so that these substitutions might not alter the structure of protein. Finally, the library was created with the variation of amino acids at positions 2, 3, 5, 10, 13, and 14 as shown the consensus comparing with DARPins in **Figure 3.1B**. All of these variable positions are localized at either in the first  $\alpha$ -helices or in the loops connecting consecutive ankyrin repeats. These positions are oriented towards the binding site of ankyrin domain as demonstrated in **Figure 3.3**. From 3D structures of

complexes of ankyrin domains with target proteins, the  $\beta$ -turns and the first  $\alpha$ -helices of protein involved in the interactions. Focusing on the distribution of amino acid at these variable positions, residues in each position from all obtained sequences were analyzed and presented as the graph in **Figure 3.4**. Proline (P) expressed very low frequency at positions 2 and 3, or absent at 5, 10, 13 and 14. Cystein (C) also presented with low proportion and did not include in these design to prevent the disulfide bonding problem. The design of degenerated codons was based on these observed natural sequences with no code for these two residues and stop codon as shown in **Table 2.1, Chapter II**. The proportion of coded amino acid of this library was shown in **Table 3.1**.

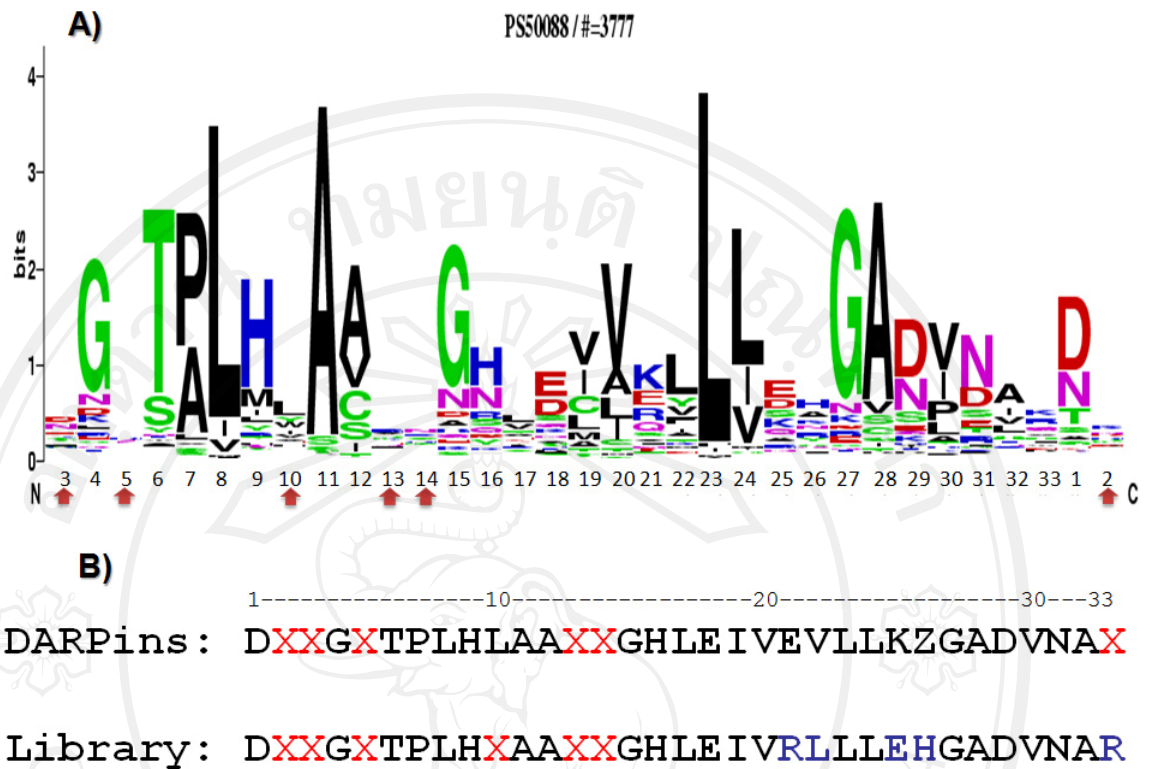


**Figure 3.1 Sequence analysis of natural ankyrin repeats.** (A) The sequence logo of natural ankyrin repeat generated from WebLogo. Amino acids are presented as single letter code. The red arrows indicate the positions for generating the artificial ankyrin library. (B) The consensus sequence of constructed library comparing with DARPin. The red letters refer to the randomized position and blue letters represent the altered residues. Recognition sites for *Bsm* BI in consensus are underlined.

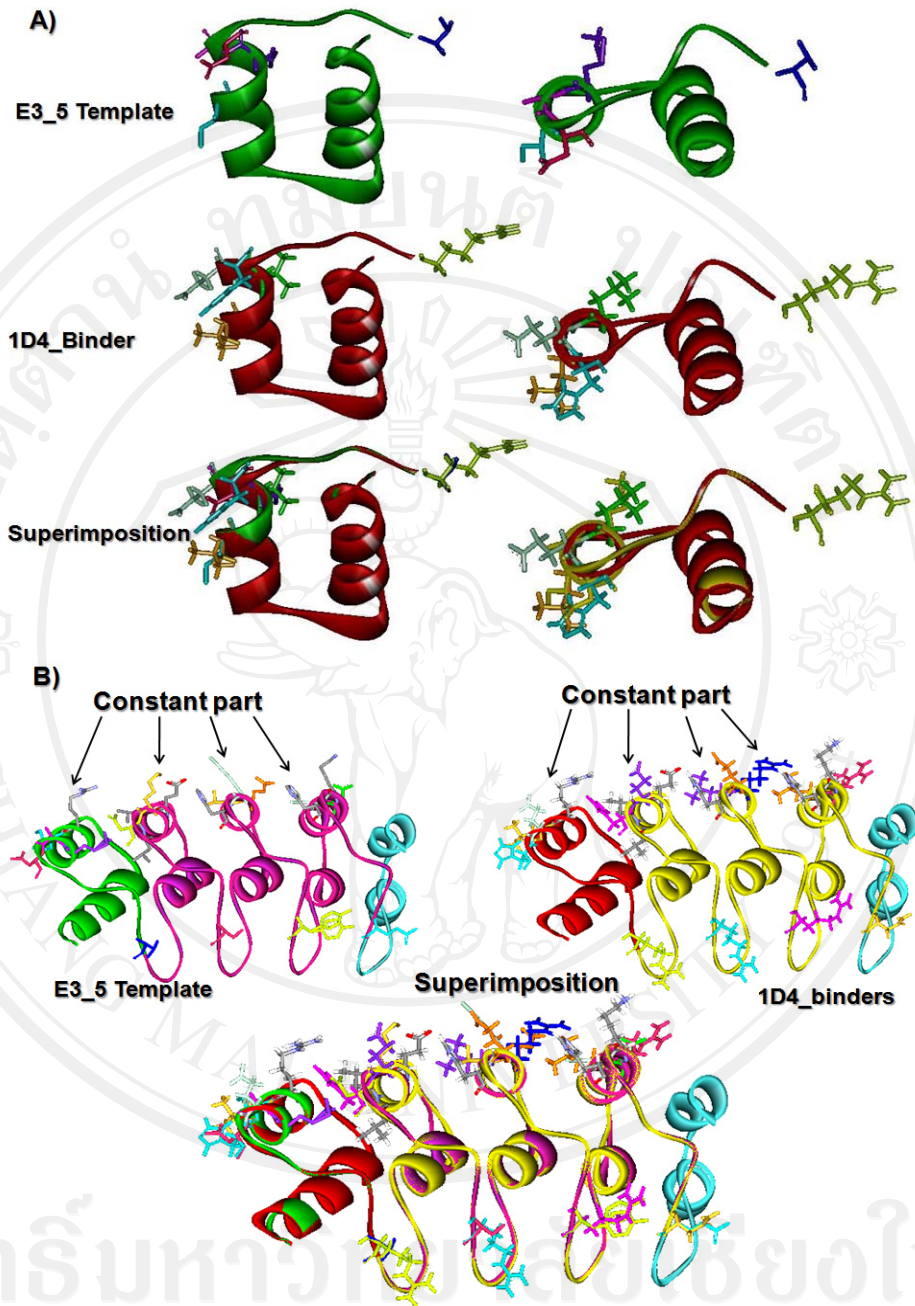


**Figure 3.2** Optimized structures of designed consensus. A single domain (A) and whole molecule of ankyrin repeat (B) are illustrated as ribbon. Substituted residues located at the constant part are depicted as stick.

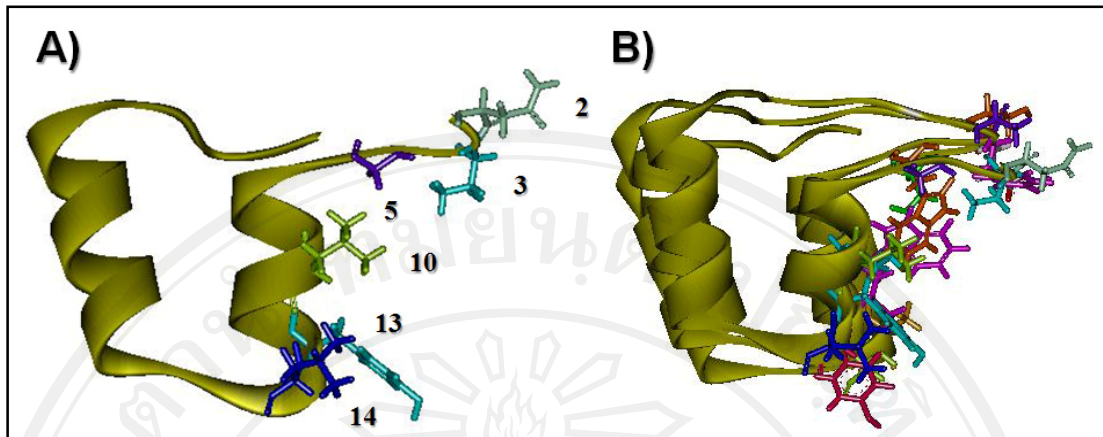


**Figure 3.3 Model structure of internal repeat.** A single repeat (A) or triple repeats (B) are presented in yellow ribbon. Amino acids at variable positions are indicated as the stick pattern.

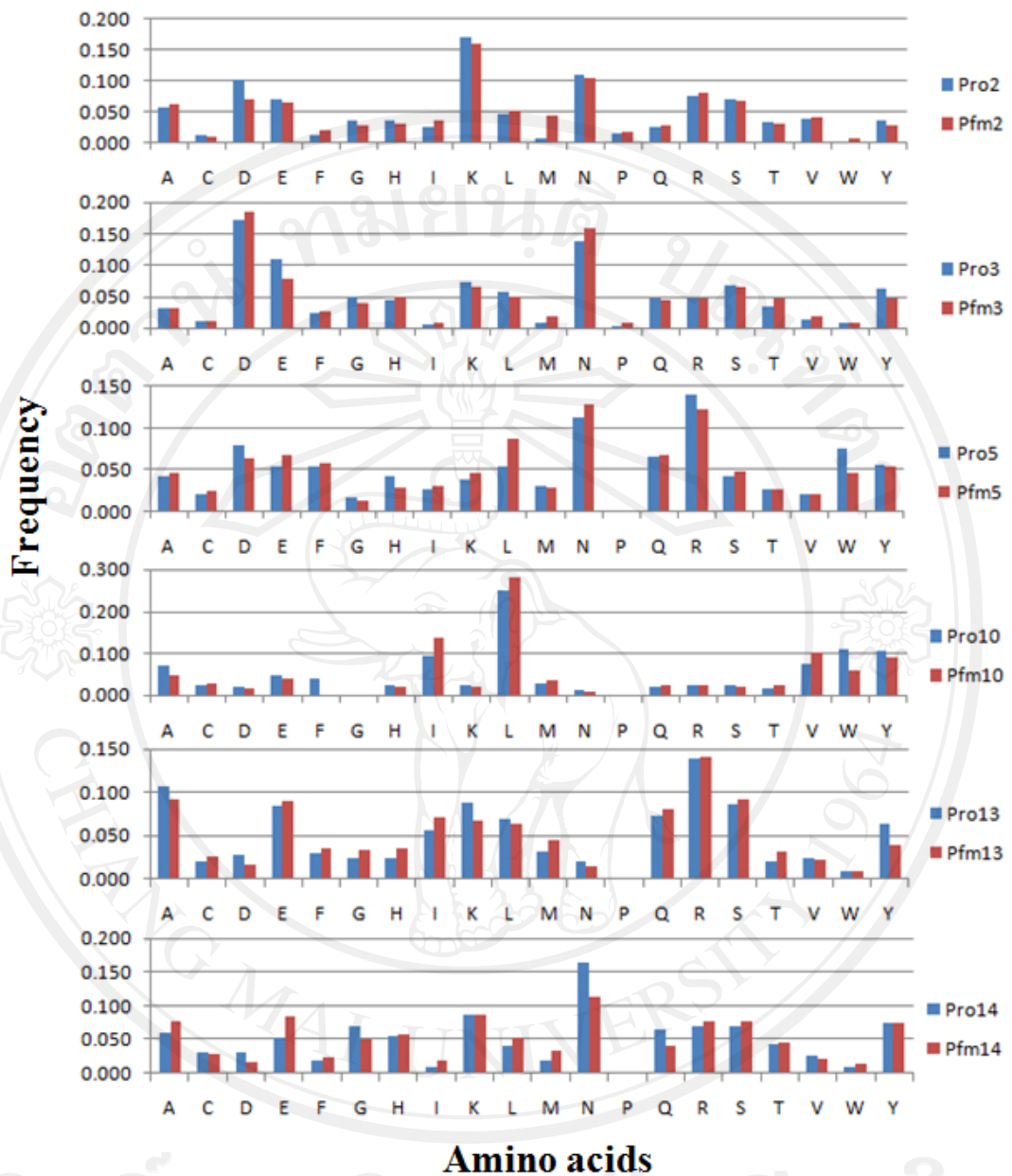


**Figure 3.4** Amino acid distribution of natural ankyrin sequences. Amino acids are presented as a single letter code. Frequency obtained from Prosite and Pfam are depicted in blue and red bar, respectively. Each graph represents the frequency at each position as indicated as the number.

**Table 3.1** Proportion of amino acid coding from mixed bases at each randomized positions.

Randomized Positions	Mixed bases*	Amino acids (single letter code)
2, 3, 5	VDK	D, E, G(2), H, I, K, L(2), M, N, R(3), S, V
	DMY	A(2), D(2), N(2), S(2), T(2), Y(2)
	RAA	E, K
	VAN	D(2), E(2), H(2), K(2), N(2), Q(2)
	TGG	W
10	CTG	L
	TGG	W
	TAC	Y
	RTC	I, V
13, 14	KCK	A(2), S(2)
	VAR	E(2), K(2), Q(2)
	SGY	G(2), R(2)
	YAY	H(2), Y(2)
	NTG	L(2), M, V

\*Mix bases refer to:  
 N= A/T/G/C  
 V= A/C/G  
 D= A/G/T  
 K= G/T  
 M= A/C  
 Y= C/T  
 R= A/G  
 S= C/G

### 3.2 Library construction

The artificial ankyrin library constructed in this study was made by a variable number of ankyrin modules with the internal variable residues flanked between N- and C-capping. The library was built using the directional polymerization of a microgene corresponding exactly to one single repeat. Polymerization was realized directly into phagemid vector as describe elsewhere (Urvoas et al., 2010). To generate this library, the defined consensus as indicated above was fragmented into four parts which were Va, Vb, Vc, and C1 (**Figure 2.1, Chapter II**). Va, Vb, and Vc encoded for amino acid positions 31-7, 8-10, and 11-17, respectively. All three fragments contained the random positions 2, 3, and 5 in Va, 10 in Vb, and 13 and 14 in Vc (**Table 2.1 Chapter II**). Constant fragment, C1, encoded for residues 18-32 with the recognition site for *Bsm* BI. All fragments were annealed with complementary bridging oligonucleotides to generate the circular DNA template coding exactly for one repeat and closed by ligation. The mixture of circularized templates was amplified using Phi 29 polymerase (Dean et al., 2001) resulting in long homopolymers of repeats that were then separated into monomers by treated with *Bsm* BI and verified by gel electrophoresis as shown in **Figure 3.5**. The monomeric fragments were polymerized directly into the treated acceptor vector (**Figure 2.3, Chapter II**). In this step, the number of modules in the library is variable and controlled by the molar ratio of acceptor vector and monomers. Consequently, the vector containing heteropolymerized repeats were subsequently captured on magnetic beads, then released from beads by *Bsp* MI digestion and finally reclosed by intramolecular ligation between the designed-compatible cohesive extremities to *Bsm*

BI. The released vectors were closed by ligation and electroporated into XL-1 Blue electrocompetent cells.

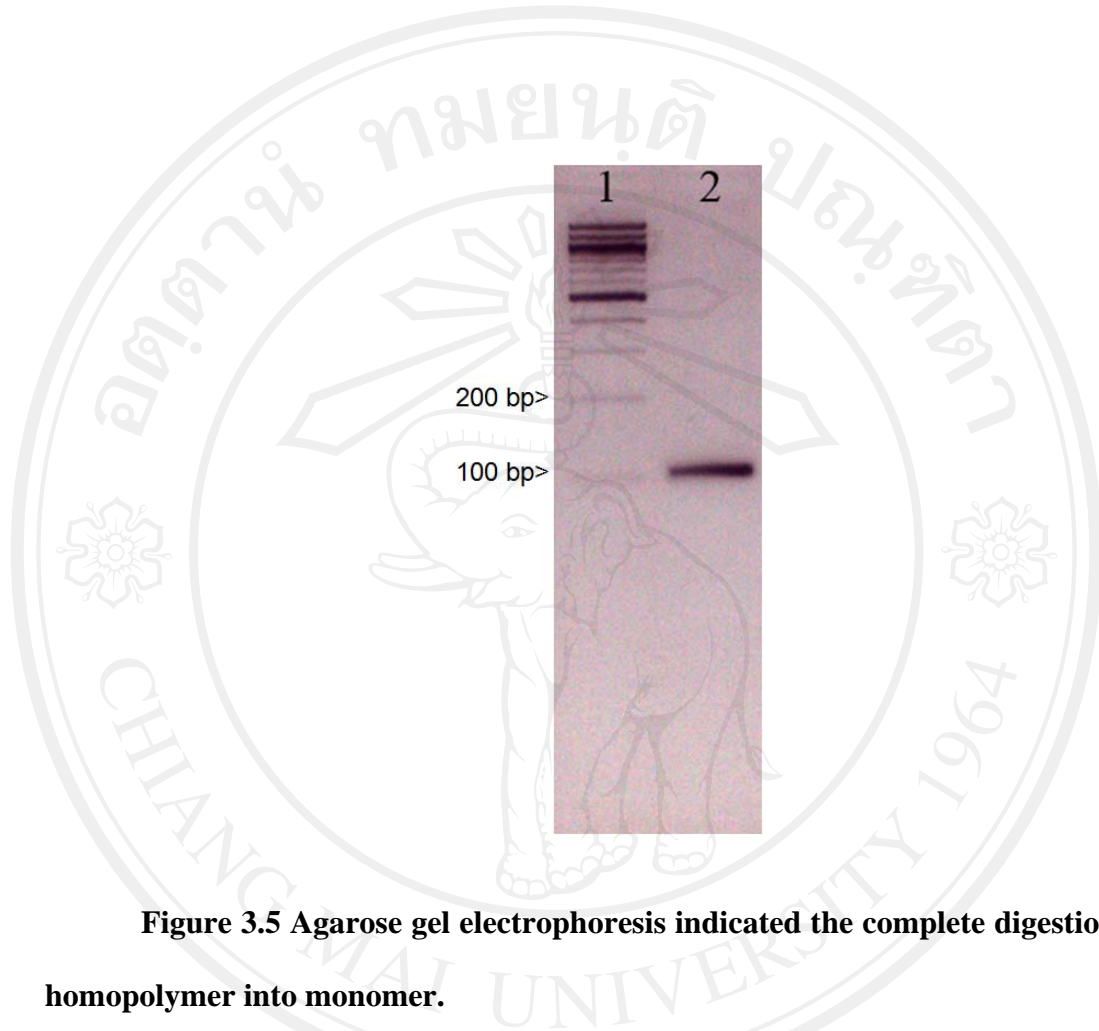


**Figure 3.5 Agarose gel electrophoresis indicated the complete digestion of homopolymer into monomer.**

Lane 1: 100 base pair DNA marker

Lane 2: Monomer of DNA coding one repeat.

### 3.3 Characterization of constructed library

An artificial ankyrin library was constructed with  $1.9 \times 10^8$  independent clones so call 'naïve library'. The distribution of repeat number was evaluated by treating plasmid pool from the library with restriction enzymes located on each side of coding sequence and separated on gel electrophoresis. As shown in **Figure 3.6A**, this result demonstrated an apparent pattern of discrete fragments certified a variation in the number of repeat between 0-15, with maximum length of 2 to 6. Sequences of thirty randomized clones were analyzed. The selected clones had the internal repeat between 1 to 5 modules, as observed the expected length by restriction analysis. Ten of these selected clones contained the coding sequence and the remaining clones had coding modules and frame-shift modules resulting in internal stop codon. These unexpected sequences could result either from oligonucleotides synthesis, or from miss-assembly and amplification as described elsewhere (Urvoas et al., 2010).

To evaluate the proportion of soluble protein expression in constructed library, a plasmid pools from library was transformed into *E. coli* BL21 (DE3) strain and 72 randomly clones were selected and evaluated soluble protein expression by colony filtration blot (CoFi blot) analysis. The positive clones were analyzed by comparing the fluorescence intensity of tested clones with that of negative control. The result revealed that 34% (24/72) of selected clones expressed soluble proteins (**Figure 3.6B**). These results suggested that the proportion of coding sequence in library is closed to that of expressing clones detected by CoFi blot. The library contains a fraction of non coding sequences which could later be a source of problems or at least of increased background in subsequent panning steps. An enrichment of coding

fraction was done by phage pre-selection or phage filtration using *Strep*-tactin® coated magnetic beads to eliminate protein-free viral particles. *Strep*-tag domain encoded upstream of ankyrin repeat fused to pIII domain of phage binds to *Strep*-tactin which is coated on magnetic beads. After phage binding step, free viral particles were washed out. Captured particles were specifically eluted using desthiobiotin and rescued by infection into *E. coli* XL-1 blue. After two round of filtration, the soluble protein expression was evaluated by CoFi blot as described. Interestingly, fraction of coding clones was enriched to 42% (30/72) and 60% (42/72) after the first and second round, respectively (**Figure 3.7**). Although, the elution step was performed using specific molecule, non coding clones still present in the filtrated library. This phenomenon could be explained by the following observations: phages are usually purified using a PEG precipitation step. Whether or not pellet resuspension of phage results to complete dissociation of multiphages aggregates is not clearly established. Washing steps are not efficient enough to completely dissociate multi phages aggregates. Non productive protein-free viral particles (bald phages) may therefore remain associated to phage actually displaying proteins. Non coding phages may therefore survive to simply select by association to protein displaying phages. In order to test the hypothesis, several option both naïve and filtrated libraries were used in parrallel to prepare phage particles for the selection process.

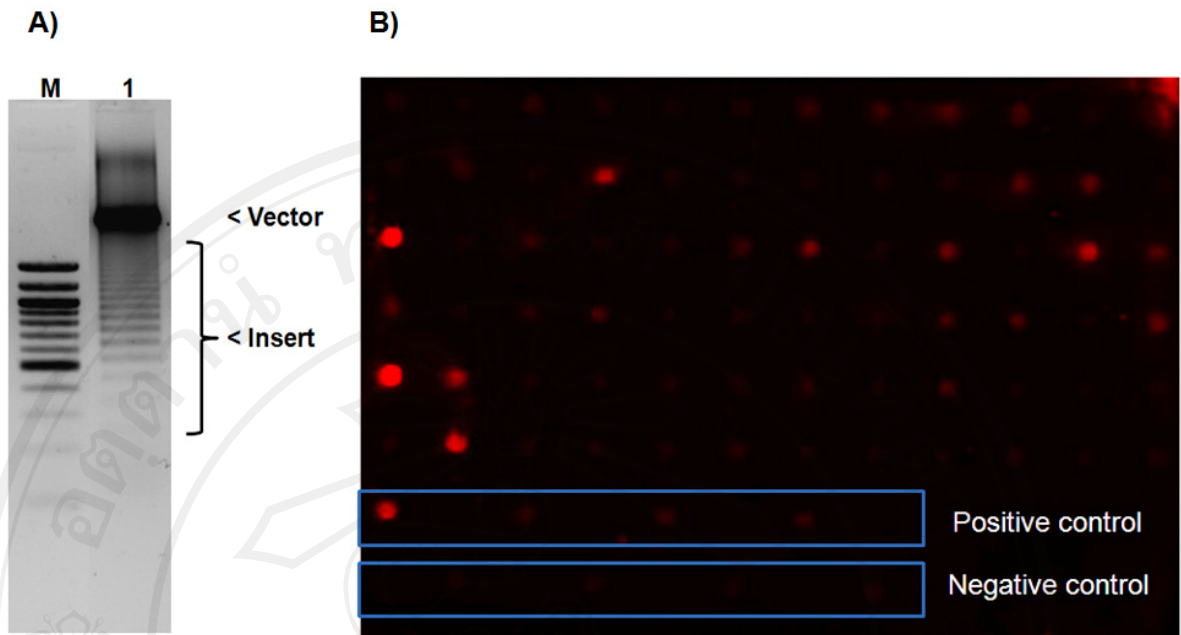


**Figure 3.6 Characterization of constructed ankyrin library.** (A) The distribution of number of repeat was evaluated by restriction analysis. Vector was extracted from plasmid pooled of library and treated with *Nde* I and *Hind* III. (B) The evaluation of soluble protein expression by CoFi blot analysis. Seventy two of randomly clones were picked up for testing. pHDiExDsbA-Ank15 and pHDiExDsbA-AccV-transformed *E. coli* were used as positive and negative control, respectively.

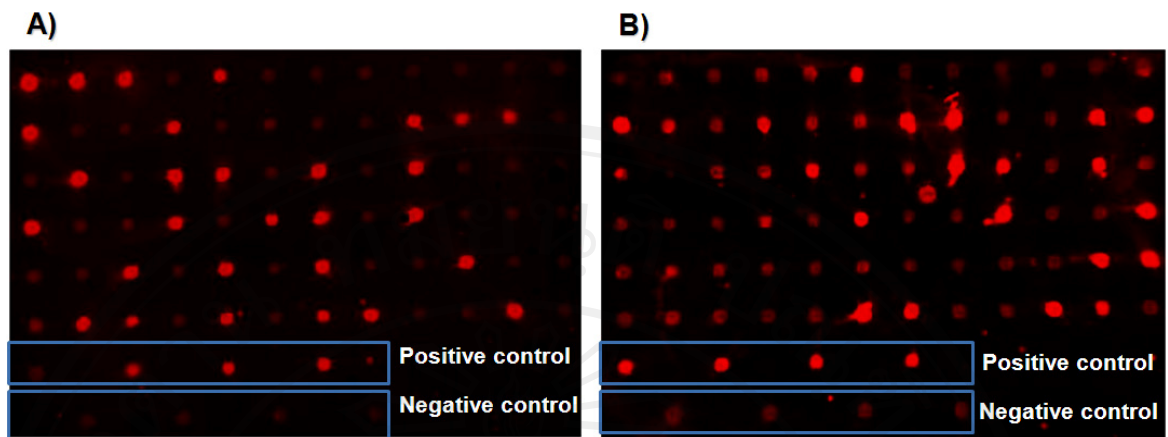


**Figure 3.7 Enrichment of coding clones by phage filtration using *Strep-tactin*® coated magnetic beads.** Seventy-two clones from first round (A) and second round (B) were randomly selected for testing the protein expression by CoFi blot. Plasmid pHDiExDsbA-Ank15 and pHDiExDsbA-AccV were used as positive and negative control, respectively.

### 3.4 Production and purification of recombinant H<sub>6</sub>MA-CA and H<sub>6</sub>-CA

The DNA fragment coding for MA-CA, a non-N-myristoylated, carboxyterminal-truncated version of HIV-1 Gag polyprotein containing the matrix (MA) and capsid (CA) domain, was cloned into *Nhe* I and *Kpn* I site of pBlueBac4.5-His resulting in pBlueBac4.5-H<sub>6</sub>MACA. This constructed transfer plasmid was co-transfected with linearized BV DNA into Sf9 cells. The recombinant BV, abbreviated BV-H<sub>6</sub>MA-CA, from transfected cells was isolated using blue plaque selection. The infected cells harboring recombinant BVs showed the blue plaque appearance after beta-galactosidase staining (**Figure 3.8A**) were picked and used for protein production. Precipitated polyhedrin was observed inside the cells infected with wild-type AcMNPV as shown in **Figure 3.8B**. The presence of recombinant H<sub>6</sub>MA-CA in the infected-cells was analyzed by Western immunoblotting using anti-His and anti-Gag antibodies. The reactive bands referring to the molecular size of H<sub>6</sub>MA-CA protein were detected in all isolated plaques as shown in **Figure 3.8C and D**. A large amount of recombinant H<sub>6</sub>MA-CA protein was produced in Sf9 cells infected with BV-H<sub>6</sub>MA-CA. Infected cells were harvested at 48 hr post infection (pi), and recombinant H<sub>6</sub>MA-CA were recovered from clarified cell lysate by Ni<sup>2+</sup>-NTA-agarose column. The recombinant protein could be isolated with high purity as shown in **Figure 3.9**. This purified protein was dialyzed against PBS and ready for isolating the binders and detecting the binding activity in the next experiments. In addition, the production of recombinant H<sub>6</sub>-CA protein was accomplished as demonstrated by detection with monoclonal anti-CA, clone M88 and G18 in ELISA and Western immunoblotting (data not shown). Cell lysate of BV-H<sub>6</sub>-CA infected Sf9 cells was subjected as antigen for proving the target compartment of selected ankyrin binders.

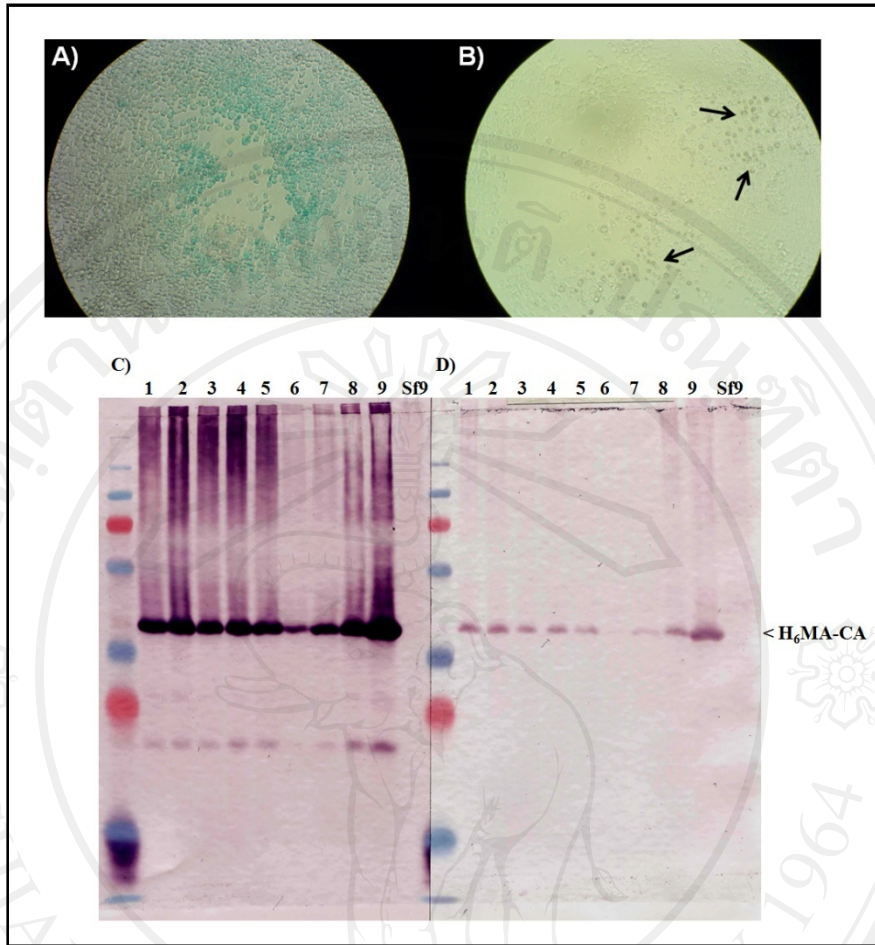


**Figure 3.8 Isolation of recombinant BV-H<sub>6</sub>MA-CA.** (A) The blue plaque appearance of Sf9 cells infected with recombinant BV-H<sub>6</sub>MA-CA. (B) The precipitated polyhedrin proteins are indicated with arrow heads of Sf9 infected with wild-type AcMNPV. Western immunoblotting results demonstrate the presence of recombinant protein in cells infected with virus from each plaques using anti-His tag (C) and anti-Gag (D) antibodies, respectively. The number indicates the given number of virus from isolated plaques. The lysate of non-infected Sf9 cell was used as negative control.

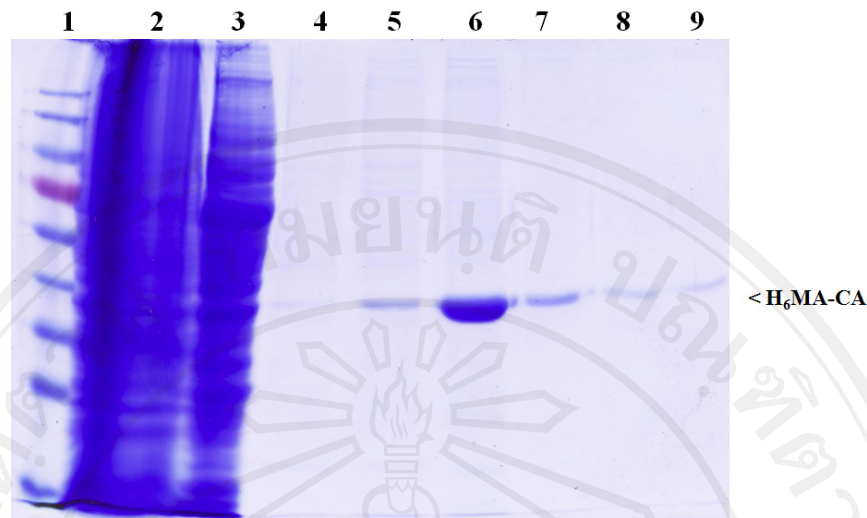


**Figure 3.9 Purification of recombinant H<sub>6</sub>MA-CA protein using Ni<sup>2+</sup>-NTA-agarose column.** Lane 1, pre-stained protein marker; Lane 2, cell lysate; Lane 3, flow-through fraction; Lane 4-9, eluted fractions. All samples were separated under denaturing conditions in 12% SDS-PAGE. The separated protein in the gel was visualized by Coomassie blue R250 staining.

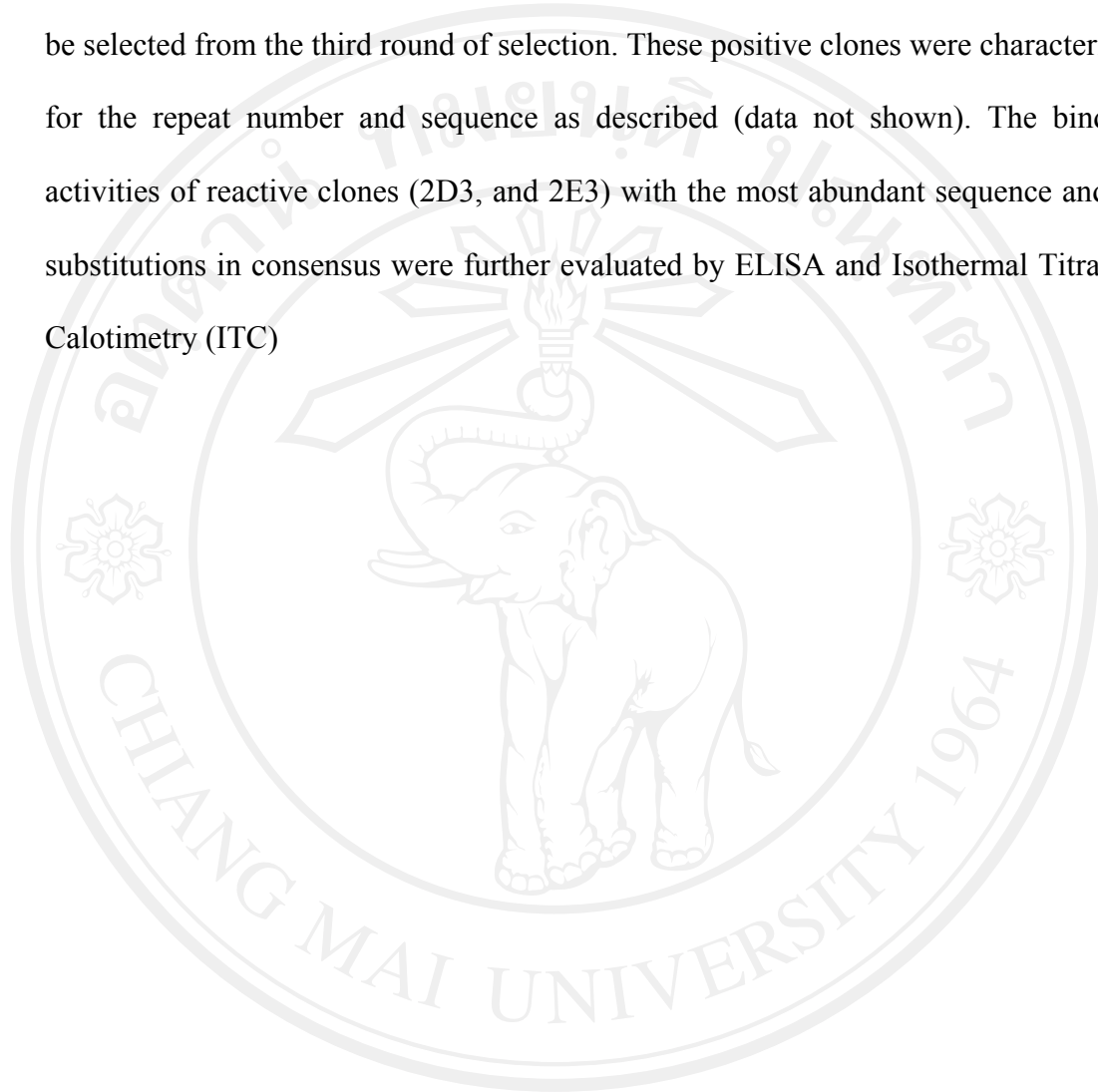
### 3.5 Isolation of H<sub>6</sub>MA-CA and A3 binders by phage selection

The phage display library used for the selection process was amplified in parallel from naïve and filtrate libraries. Furthermore, in order to evaluate effects of phage precipitation on the outcome of selection, phage stock were prepared either using a conventional PEG precipitation step or directly from culture supernatant without any precipitation process. The phage titration from the first round of selection showed that precipitated phages from both naïve and filtrate library had background 10 times over the phage from supernatant while the number of phage input and output were found at the same number. This finding guided us to use the phage without precipitation to lower the background in the next round of selection. Phage screening was performed after the second round of selection. Focusing on H<sub>6</sub>MA-CA binders, interestingly, one reactive clone of five tested clones was detected from the filtrate library after the first round of selection. Moreover, a higher proportions of positive clones was observed from filtrate library (10 of 33) comparing with that from naïve library (4 of 32) as shown in **Figure 3.10A**. To further performing the third round of selection, phages input were amplified from a pool clone of eluted phages from the filtrate library. In addition, to recover the specific binders, soluble antigen was used for elution instead of using acid solution. Released phages were collected at different time points. Randomized clones of each eluted fractions were selected for phage screening as shown in **Figure 3.10B**. Almost 70% of clones in all elute fractions produced a binding signal significantly over the background. All positive clones from the first and second round, and the top five clones of each elute fractions in third round which showed the highest binding activity were examined for the number of repeat by restriction analysis. Most of selected binders (32 of 39) contained 2 internal

repeats as shown by the molecular size (370 base pairs). Other binders contained 3 repeats as indicated by the size at 470 base pairs (**Figure 3.11**). Positive clones were sequenced by standard sequencing method. Selected binders were divided into two major groups depending on the number of internal repeats. In the group containing two repeats (**Figure 3.12A**), a first subgroup includes four identical sequences found from the first and second round of selection (1A9, 1A12, 1C12, 1, and 1D10). Another clone, 1D3, had nine different amino acids located in variable positions. Reactive candidates from third round were classified in three groups. 6A5, 7F7, and 6D12 have the same sequences as the first group at variable positions but different amino acids in consensus. Sequences of three clones, 6E9, 7D11, and 7G7, hold some different positions in consensus and the most of random positions. Another group, 7A8 and 7C6, also differ in some positions in consensus and five residues in variable positions. Focusing on group containing three repeats (**Figure 3.12B**), four groups could be classified. Clone 1B4, 1B8, and 1D8 displayed the most abundant sequences where as clone 1D4, 6B4, and 6G5 had individual sequence. Interestingly, the most observed amino acid substitutions (E17K, V18F, D28E) in N-capping repeat occurred in the consensus of binders selected from the third round. Finally, clones containing three internal repeats without substitutions in consensus, 1B8, and 1D4, and also 6B4 were selected to investigate the binding activity *in vitro*.

In this study, A3 protein was also used as a target molecule for evaluating this constructed artificial ankyrin repeat for its ability to select specific binders. This protein is an artificial alpha-helical repeat protein ( $\alpha$ Rep) based on thermostable HEAT-like repeats as described (Urvoas et al., 2010). It's also folded cooperatively and is very stable. Reactive binders could be isolated. Five of 33 tested clones from

naïve library after the first round of selection gave a positive signal. No of positive clone was found from filtrate phage (data not shown). Moreover, many binders could be selected from the third round of selection. These positive clones were characterized for the repeat number and sequence as described (data not shown). The binding activities of reactive clones (2D3, and 2E3) with the most abundant sequence and no substitutions in consensus were further evaluated by ELISA and Isothermal Titration Calorimetry (ITC)



ลิขสิทธิ์มหาวิทยาลัยเชียงใหม่  
Copyright© by Chiang Mai University  
All rights reserved

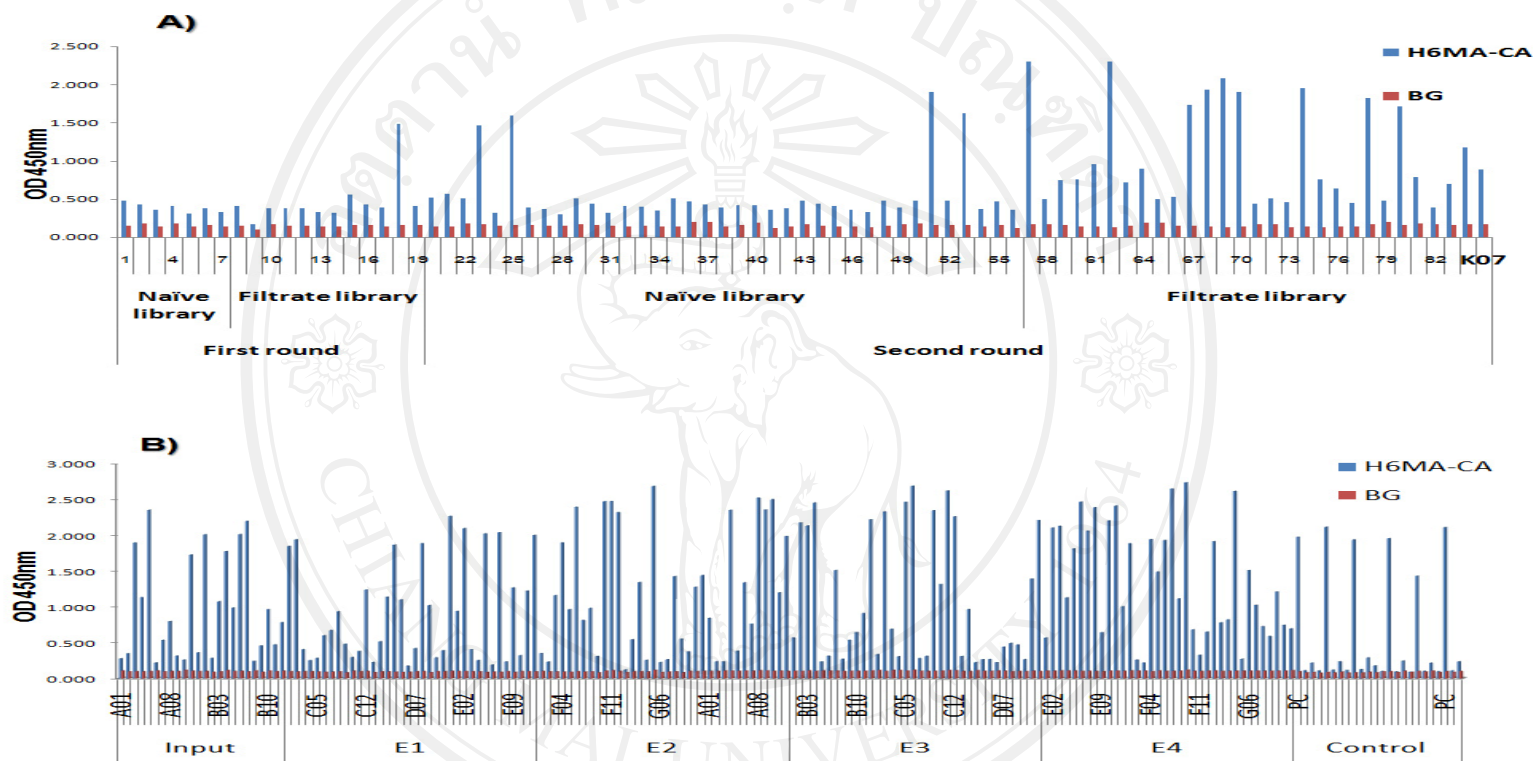


**Figure 3.10 Phage ELISA for screening of the H<sub>6</sub>MA-CA binders.** Culture supernatants containing phage particles from first and second round of selection (**upper panel**) and third round selection (**lower panel**) were added into H<sub>6</sub>MA-CA coated wells and un-coated wells (BG). The bound phages were traced with HRP-conjugated anti-M13 antibody. The signal was measured at 450 nm after developing the TMB substrate. The positive and negative clones of the first round were used as control in the screening of third round. The sequential elution of third round selection using free H<sub>6</sub>MA-CA is indicated as E1, E2, E3, and E4.

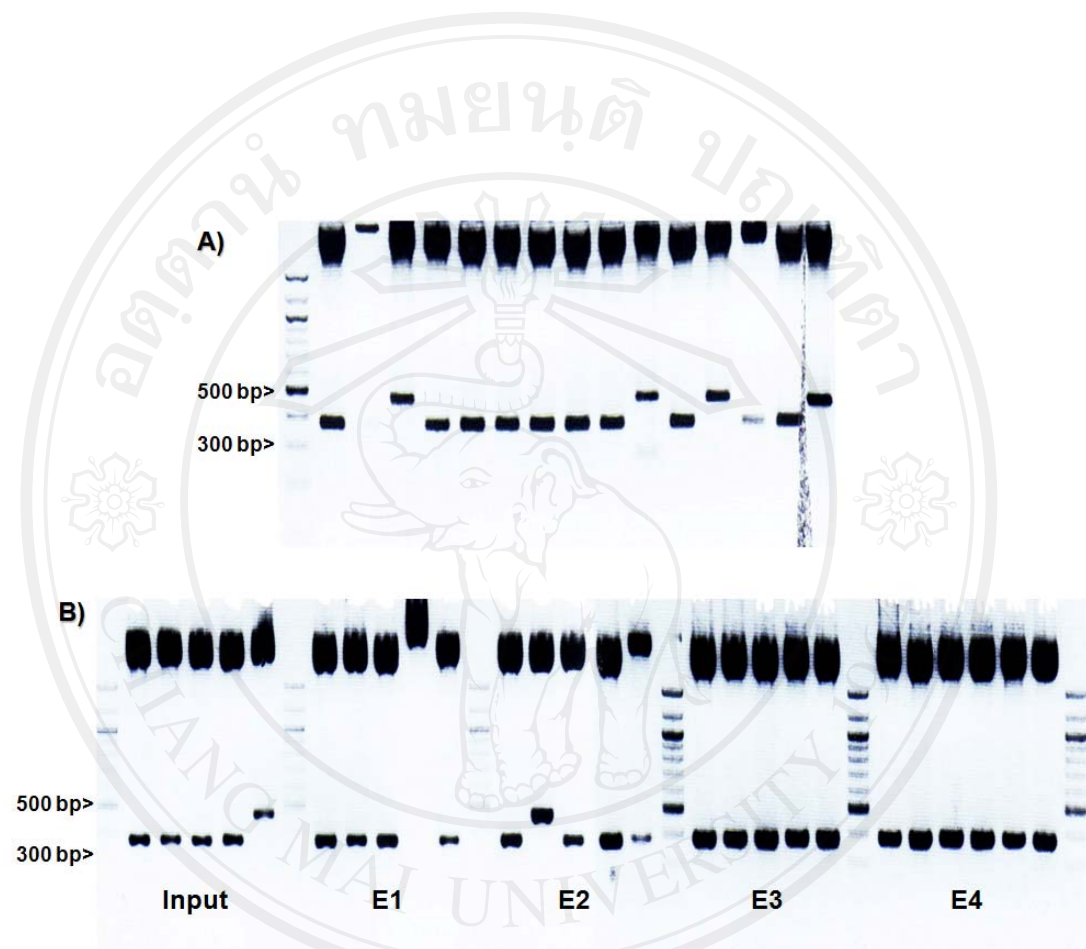


**Figure 3.11 Distribution of repeat number of selected H<sub>6</sub>MA-CA binders.** Plasmids were extracted from positive clones of first and second round (A), and third round (B) of selection and double treated with *Not* I and *Hind* III. Treated vectors were analyzed by gel electrophoresis. Clones from sequential elution are indicated as input, E1, E2, E3, and E4, respectively.

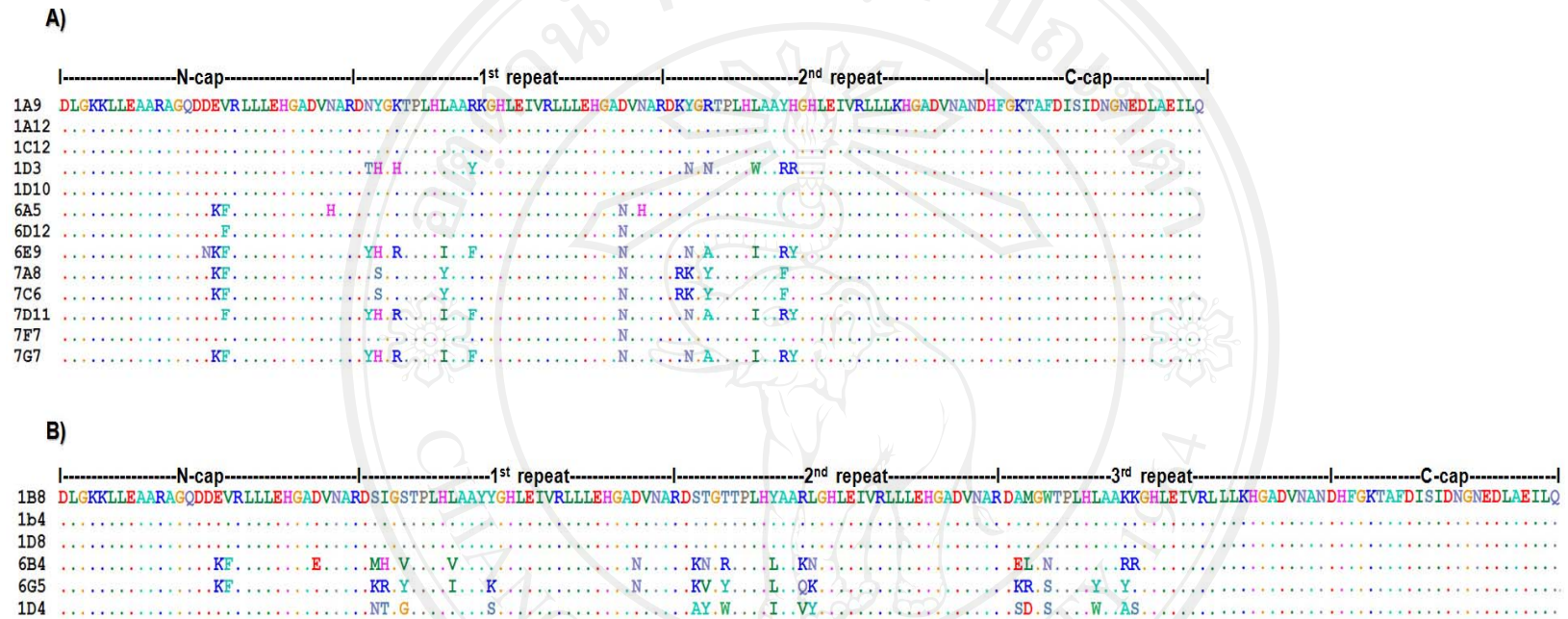


**Figure 3.12 Sequence analyses of H<sub>6</sub>MA-CA binders.** Selected binders were analyzed the sequence and divided into two groups depending on their internal repeat number, two repeats (**A**) and three repeats (**B**).

### 3.6 Generation of monoclonal antibodies against H<sub>6</sub>MA-CA

The titers of polyclonal antibodies against H<sub>6</sub>MA-CA after the third immunization from mice were determined by indirect ELISA. Polyclonal antibodies of mouse A had a higher signal than that of mouse B at the same dilution without any background (**Figure 3.13**). Spleenocytes of mouse A were collected to generate the hybridoma cells. The culture supernatants from wells containing hybridoma cells were collected and screened for antibody reactivity by ELISA and Western immunoblotting.

Culture supernatants of 278 clones were screened for their reactivity by ELISA. As shown in **Figure 3.14A**, thirteen of all tested clones showed a high signal over the background demonstrating the reactivity of secreted antibody from hybridoma clones but other clones expressed no significant signal over background (data not shown). All positive clones were further characterized for their epitope by Western immunoblotting (**Figure 3.14B**). Cell lysate of BV-H<sub>6</sub>MA-CA infected cells were separated and transferred to the PVDF membrane. Anti-His tag and anti-Gag were used to localize the molecular size of H<sub>6</sub>MA-CA fusion protein and partially cleaved form of H<sub>6</sub>MA at ~40 kDa and ~17kDa, respectively. No reactive band was observed on membranes reacted with the following clones: G106, M7, M8, M25, G57, M68, and M102 suggesting that these clones bind to a conformational epitope. Other clones, G46, G52, G53, and M48 exhibited 2 positive bands (~40 kDa and ~17kDa) indicating their epitope presented on MA domain. Furthermore, clones G18, and M88 bind to CA domain as revealed by two reactive bands at ~40 kDa and ~24 kDa.

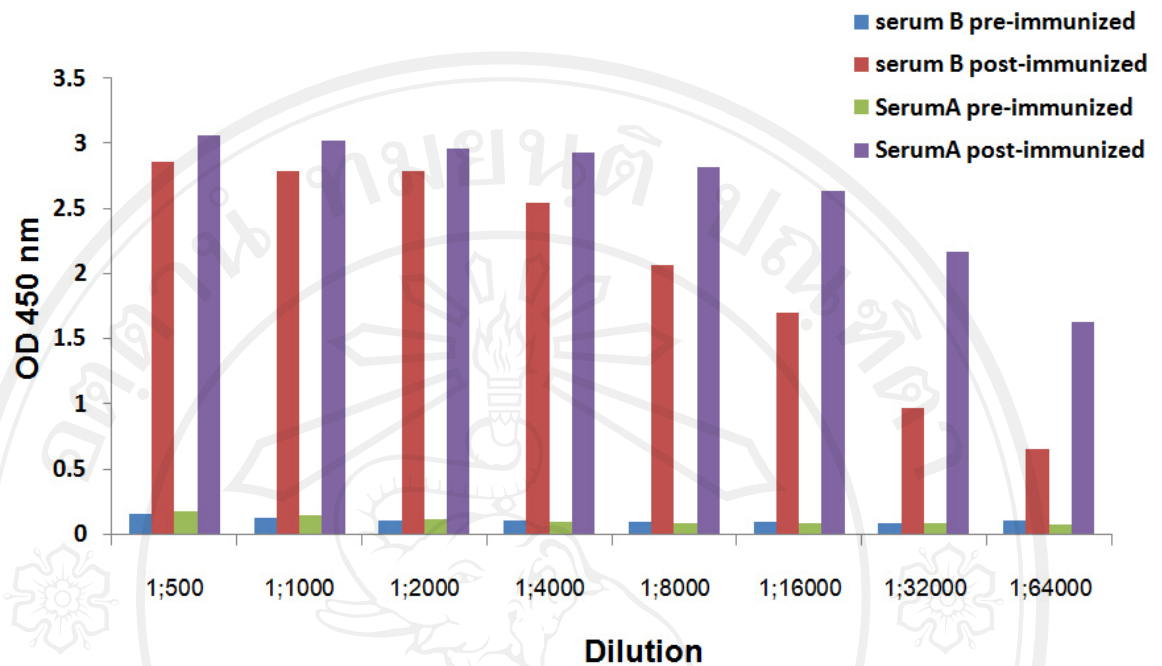


**Figure 3.13** The reactivity of polyclonal antibodies in immunized mice serum. The serial diluted sera were collected after third immunization and determined for the antibody reactivity by indirect ELISA. The pre-immunized sera were tested at the same time.

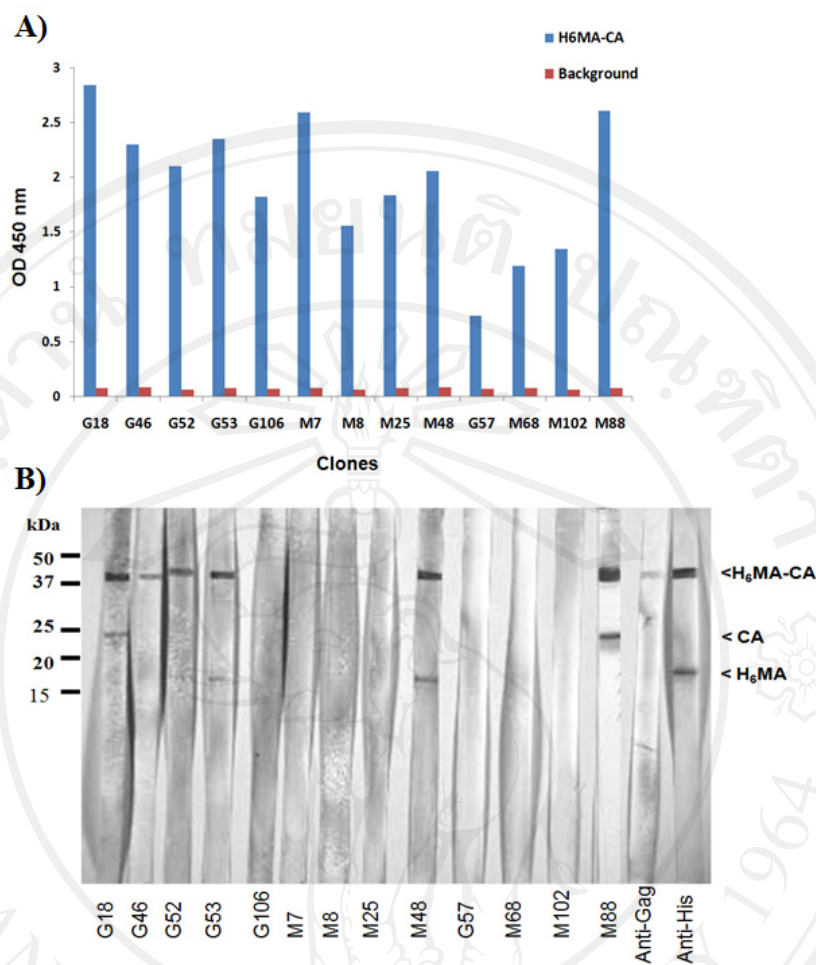


**Figure 3.14 Characterization of antibody reactivity.** (A) Culture supernatants from hybridoma clones were added into H<sub>6</sub>MA-CA coated wells. The captured antibodies were detected by HRP-conjugated goat anti-mouse immunoglobulins and signals were measured at 450 nm after adding substrate and HCl. (B) Cell lysate of infected cells was separated and probed with culture supernatants. The bound antibodies on membrane were revealed by HRP-conjugated goat anti-mouse immunoglobulins. The picture was captured after adding TMB membrane substrate. The molecular sizes of recombinant proteins are indicated.

### 3.7 Binding activity of selected ankyrin binders

Three clones of reactive binders were first chosen to evaluate the binding activity *in vitro*. Gene coding for these binders were cut from phagemid vector and subsequently cloned into pQE-30 expression vector for high level of protein expression in *E. coli* M15 [pREP4] strain. Ankyrin binders were expressed and purified using HisTrap column followed by size exclusion using Sephadex G-75. The purity of purified ankyrin binders were evaluated in 15% SDS-PAGE under reducing condition with high amount of protein and stained by Coomassie's blue staining (**Figure 3.15A**). Ankyrin binders and H<sub>6</sub>MA-CA protein hold the same tag which might limit the detection in ELISA-based method. Purified ankyrin binders were chemically biotinylated using EZ-Link Sulfo-NHS-LC-Biotin kit and verified by dot blot (**Figure 3.15B**). Three selected candidates could be conjugated with biotin as shown by the blue color developed from the reaction in the second membrane as compared with no signal with non-biotinylated protein.

The reactivity of biotinylated binders was assessed by dot blot analysis (**Figure 3.16A**). H<sub>6</sub>MA-CA or A3 coated on membrane were reacted with biotinylated proteins and subsequently traced by HRP-conjugated extravidin. Reactive dots were visualized by adding HRP substrate (TMB) to the membrane incubating solution. As shown in **Figure 3.16A**, blue dots were observed only at H<sub>6</sub>MA-CA. This result indicated that ankyrin binders kept their binding activity after biotinylation and also expressed the specificity to their antigen. To confirm the specific interaction, biotinylated binders were mixed with its non-biotinylated form and irrelevant binders (2D3, the A3 binder) and then added into H<sub>6</sub>MA-CA coated wells. The bound-

biotinylated binders were detected by reacting with HRP-conjugated extravidin. Interestingly, as presented in **Figure 3.16B**, the inhibition could be observed in the mixture of biotinylated-protein with its free form (blue bar) while irrelevant ankyrin showed not significant effect (red bar). This result confirmed that, all three selected binders bound to their target molecule. Moreover, 1D4 exhibited the highest signal follow by 1B8, and 6B4 respectively.

Furthermore, competitive ELISA was done to evaluate the specificity of selected binders with various inhibitors. As resulted in **Figure 3.17**, the inhibition effect was observed while ankyrin clones 1B8, 1D4, 6B4 were used as inhibitors for biotinylated-1B8, and -1D4 but not ankyrin clone 2E3 which is A3 binders. These results indicated that all binders might react at the same or nearby area on target protein. Remarkably, clone 1D4 represented the highest binding signal with the target protein (blue bar, no inhibitor) and exhibited the best inhibiting effect. This clone was, hence, chosen for evaluating its binding activity by ITC method. Additionally, the binding activity of these binders was evaluated by performing sandwich ELISA using monoclonal antibodies against CA domain (**Figure 3.18C, upper panel**). Biotinylated-ankyrin 1D4 and 1B8 could bind to the captured-target protein on the well (**Figure 3.18C, lower panel**). These results confirmed the binding reaction in previous experiments. Besides, Biotinylated-antibodies also exhibited the binding activity on both antibodies-coated wells indicating that these two antibodies bind to different epitopes or the multiple recognition sites presented on the wells.

The epitope localization of ankyrin binders was analyzed by western immunoblotting as described. Clones 1B8, 1D4, and 6B4 reacted to the separated proteins on membrane and provided a positive band at molecular size of H<sub>6</sub>MA-CA

but not at H<sub>6</sub>MA (**Figure 3.18A**). The indirect ELISA using H<sub>6</sub>-CA recombinant protein captured on Ni-coated wells was performed to confirm the recognition epitope of these three ankyrin binders. Positive signals were detected with all H<sub>6</sub>MA-CA binders (1B8, 1D4, and 6B4) but not A3 binder (2D3) (**Figure 3.18B**). This result indicated that, the epitope of these three H<sub>6</sub>MA-CA binders was situated in the CA domain.

Additional confirmation of affinity and specificity was obtained from isothermal titration calorimetry (ITC) experiments. Titration of increasing amounts of 1D4 into sample cell containing purified H<sub>6</sub>MA-CA provided a dissociation constant ( $K_d$ ) of 0.45  $\mu$ M (**Figure 3.19A**). ITC also confirmed specificity, as 1D4 binding to A3 was not detected in this assay (**Figure 3.19B**) whereas 2D3 reacting to A3 exhibited a  $K_d$  of 18 nM (**Figure 3.19C**). These data also validated the competition assays as an accurate measurement of affinity. Moreover, the useful obtained data from a single ITC experiment was the stoichiometry (N) which deals with the quantitative relationships between protein and its ligand or the number of binding sites. From the fitting curve, the calculated stoichiometry value was 0.656 indicating the molar ratio of H<sub>6</sub>MA-CA and 1D4 was around two. This finding supported the result of sandwich ELISA. The result would be explained by the dimerization of this protein (**Figure 3.19D**) as described in previous study (Gamble et al., 1997) resulting in the multiple recognition site presented on the wells.

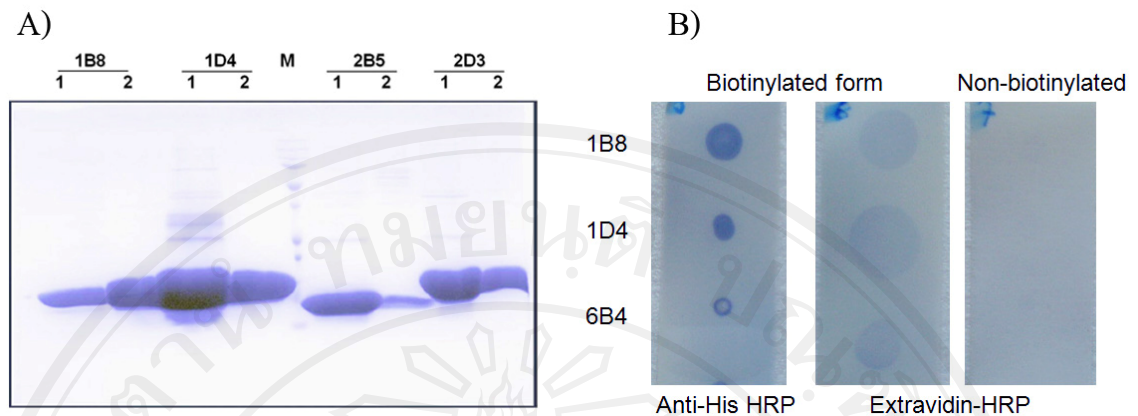


**Figure 3.15 Production and biotinylation of purified ankyrin binders.**

Ankyrin binders were expressed in *E. coli* and purified using two step; HisTrap column (A, Lane 1 of each clone) followed by size exclusion column (A, Lane 2 of each clone). Purified proteins were chemically linked with biotin and verified by dot blot analysis (B) using HRP conjugated anti-His and extravidin. The same amount of non-biotinylated protein was used as control.

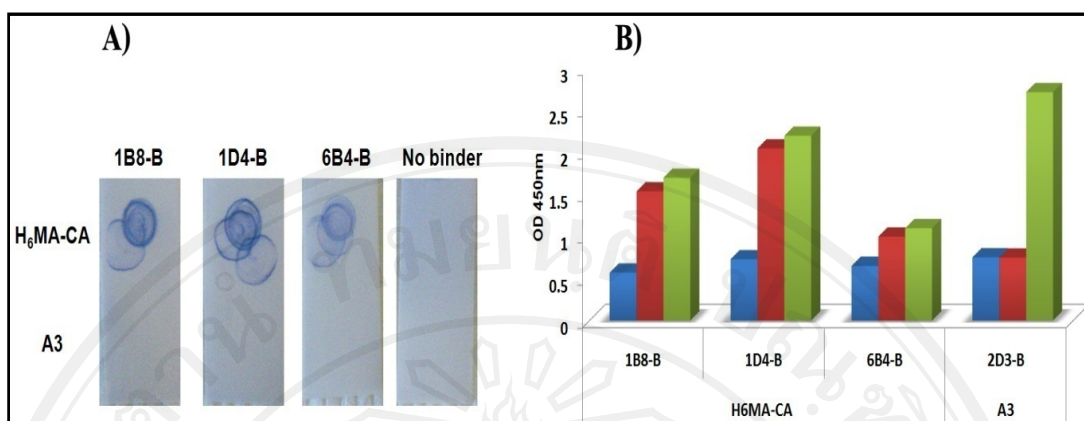


**Figure 3.16 Binding activities of biotinylated ankyrin binders.** (A) Dot blot analysis. Biotinylated-ankyrin binders were reacted with H<sub>6</sub>MA-CA and A3 coated on membrane. The reactive dots were developed by revealing membrane with HRP-conjugated extravidin and followed by adding precipitating substrate. (B) Competitive ELISA. The mixture of biotinylated-binders with its free form (Blue bars), with irrelevant ankyrin binders (Red bars), and with no inhibitor (Green bars) were added into H<sub>6</sub>MA-CA- or A3-coated wells as indicated. Bound-ankyrin binders were detected by adding HRP-conjugated extravidin. The signal was measured after TMB substrate developing.

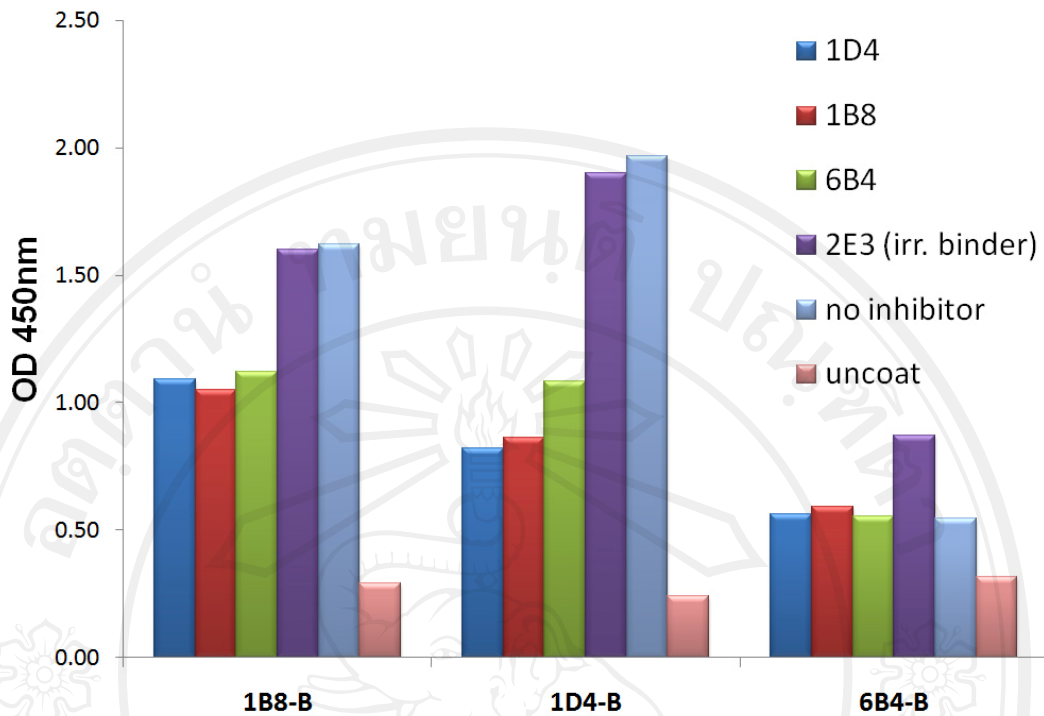


**Figure 3.17 Specific reactivity of ankyrin binders.** The binding of Biotinylated-ankyrin binders were inhibited with various inhibitors including free H<sub>6</sub>MA-CA binders (1D4, 1B8, and 6B4). A3 binder (2E3) was used as negative control.

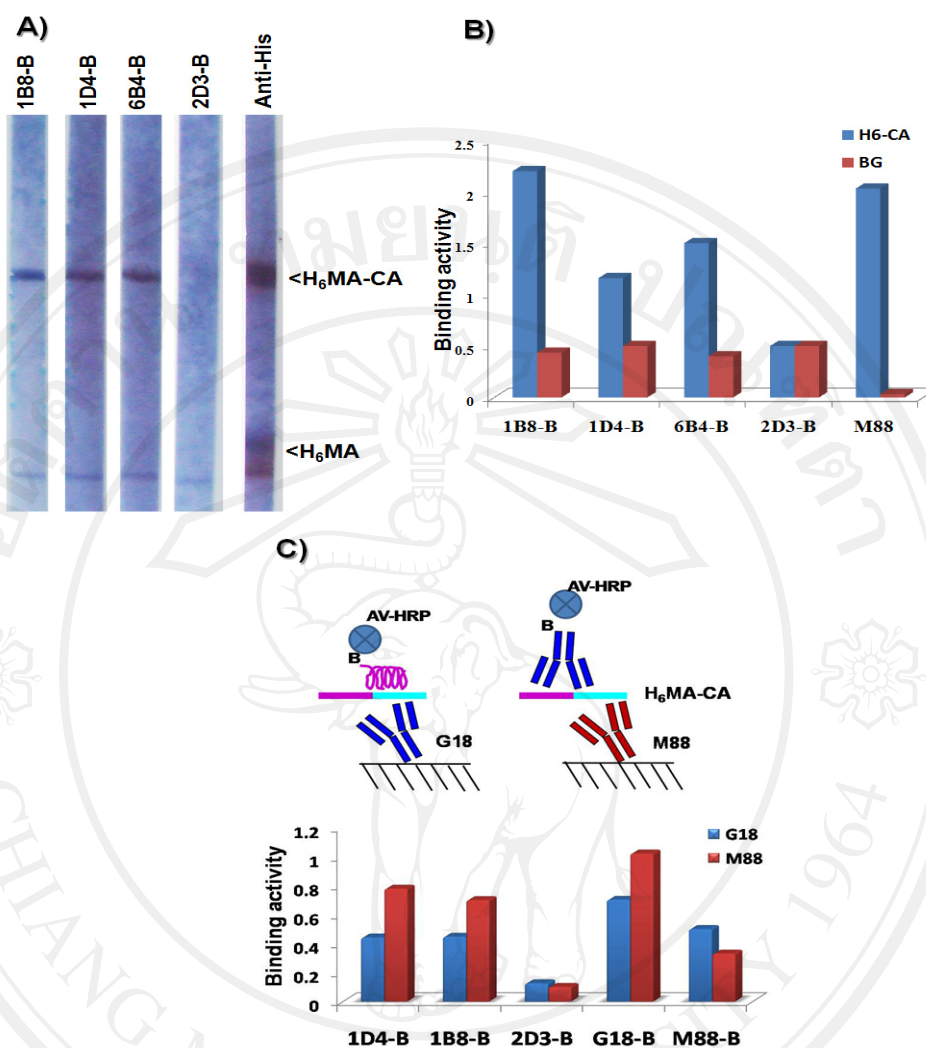


**Figure 3.18 Epitope localization of selected binders.** (A) Binding reactivity of ankyrin with cell lysate of BV-H<sub>6</sub>MA-CA blotted membrane. Anti-histidine tag was used for indicating the molecular size of target protein. (B) Indirect ELISA of H<sub>6</sub>-CA captured on Ni-treated plate. Monoclonal anti-CA (clone M88) and ankyrin 2D3 were used as positive and irrelevant binder control. (C) Schema demonstrating the sandwich ELISA, upper panel. The binding reactivity of biotinylated-binders reacting with the antibody-captured H<sub>6</sub>MA-CA on the wells, lower panel and with the cell lysate of BV-H<sub>6</sub>MA-CA blotted membrane.

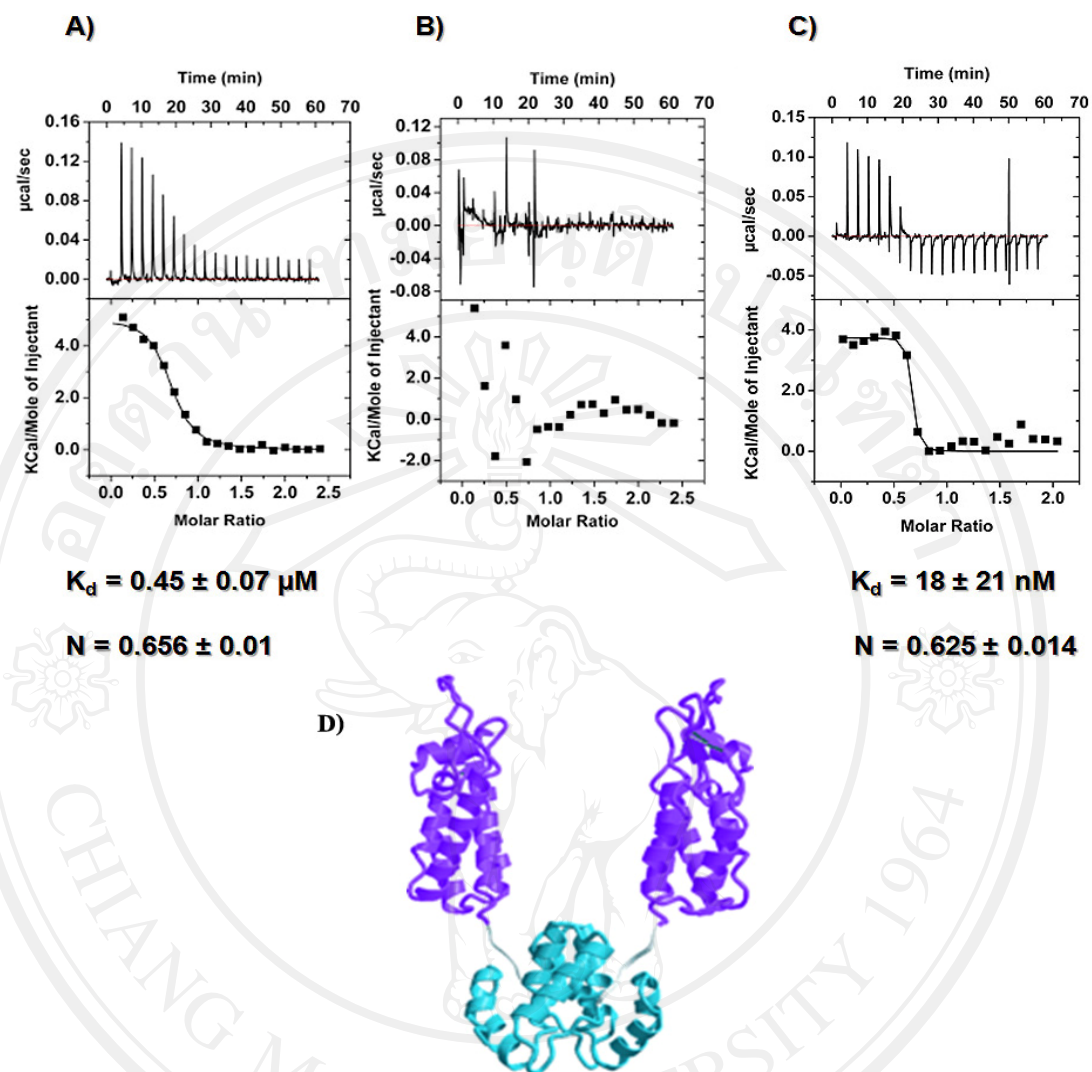


**Figure 3.19** Affinity and specificity of selected ankyrin binder. ITC

experiment was performed to measure the binding activity of 1D4 with H<sub>6</sub>MA-CA (A), 2D3 with A3 (C), and to evaluate the specific binding of 1D4 (B). The picture represented model for the intact HIV-1 capsid dimer (D). The CA(146–231) dimer (cyan) is shown covalently linked to the CA(1–151) domain (Gamble et al., 1997)

### 3.8 Hindrance of HIV-1 maturation by interfering protease activity

HIV-1 protease plays a key role in viral maturation by cleavage of the nascent polypeptide into mature proteins. In our lab, we have developed a method based on ELISA to detect the activity of HIV-1 protease and its variants by taking the advantage of antibody against C-terminus of MA domain, anti-p17, (manuscript is in preparation). In this study, this method was applied to assess the interfering effect of selected ankyrin binders to block the cleavage process. H<sub>6</sub>MA-CA protein captured on nickel-treated plate was reacted with ankyrin binders before treating with HIV-1 protease. The cleaved form of substrate was evaluated by detecting the presence of C-terminus of MA. As shown in **Figure 3.20**, a positive signal was observed as same as noinhibitor control. The result indicated that all three selected clones exhibited no interfering effect on HIV-1 protease activity

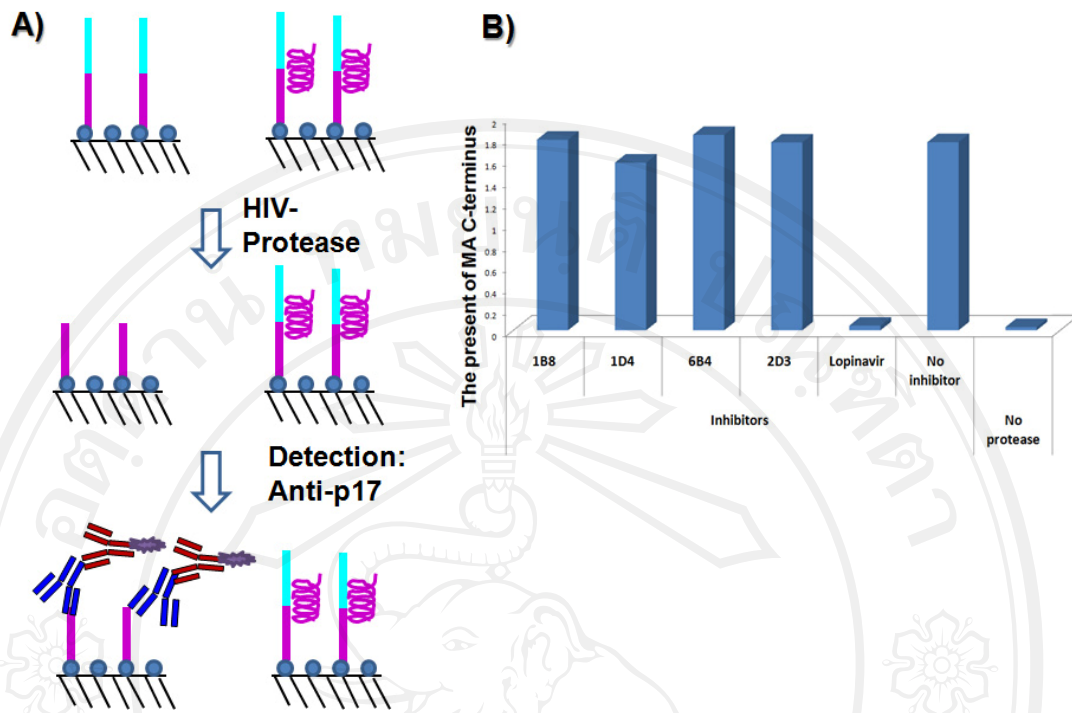


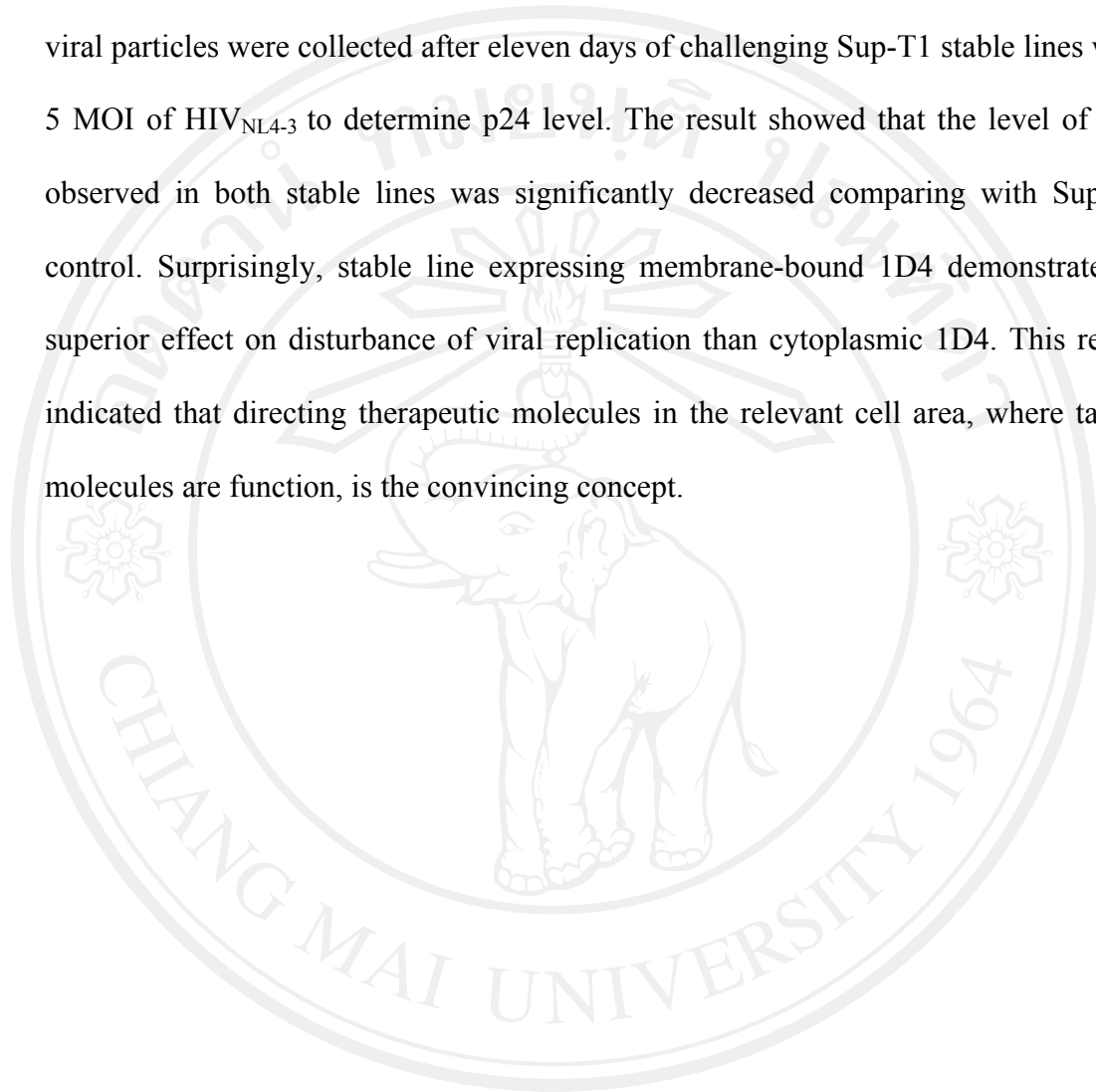
**Figure 3.20 Interference of HIV-1 protease activity by selected ankyrin binders.** (A) Schematic represents ELISA system for testing the protease activity. H<sub>6</sub>MA-CA-captured on microwells were reacted with or without ankyrin binders before treatment with protease. The cleaved form of substrate was detected using monoclonal anti-p17 and subsequently traced by goat anti-mouse IgS conjugated HRP. (B) Interfering effect of selected ankyrin binders on HIV-1 protease activity. Lopinavir was used as a protease inhibitor control.

### 3.9 Intracellular function of ankyrin protein on viral assembly

DNA fragment encoding ankyrin binder clone 1D4 was amplified using two sets of primers to generate two versions of expression vectors. Each product was subsequently submitted to overlapping PCR with the gene coding for green fluorescence protein (GFP) which is used as a reporter and then subcloned into pCEP4-based vector. The resulting vectors are pCEP4Myr1D4-GFP containing myristoylation signal at N-terminus of ankyrin for targeting protein to the membrane and pCEP4Cyt1D4-GFP for cytoplasmic expression (**Figure 3.21**). For the establishment of stable lines, these two vectors were separately transfected into SupT1 cell line. pCEP4-based plasmid is an episomal mammalian expression that uses the cytomegalovirus (CMV) immediate early enhancer/ promoter for high level transcription of recombinant genes. Epstein-Barr Virus replication origin (oriP) and nuclear antigen encoded by this plasmid permit extrachromosomal replication in mammalian cells. Moreover, this vector also carries the hygromycin B resistance gene for stable selection in transfected cells. Thus, in this experiment, transfected cells were maintained in medium containing hygromycin B.

The stable cells were observed for the protein expression under the fluorescence microscopy (**Figure 3.22A**) and flow cytometer (**Figure 3.22B**). Interestingly, myristoylation signal efficiently directed the GFP-fused ankyrin protein to the membrane as shown by the green fluorescence located at the plasma membrane (**Figure 3.22A upper panel**). In contrast, non-myristoylated ankyrin diffused throughout the cells (**Figure 3.22B, lower panel**). Additional data from flow cytometry demonstrated that 95% GFP positive cells were observed with both stable

lines. These results indicated that most of the cells expressed ankyrin protein and could be used to evaluate its intracellular function. Culture supernatants containing viral particles were collected after eleven days of challenging Sup-T1 stable lines with 5 MOI of HIV<sub>NL4-3</sub> to determine p24 level. The result showed that the level of p24 observed in both stable lines was significantly decreased comparing with Sup-T1 control. Surprisingly, stable line expressing membrane-bound 1D4 demonstrated a superior effect on disturbance of viral replication than cytoplasmic 1D4. This result indicated that directing therapeutic molecules in the relevant cell area, where target molecules are function, is the convincing concept.



ลิขสิทธิ์มหาวิทยาลัยเชียงใหม่  
Copyright© by Chiang Mai University  
All rights reserved

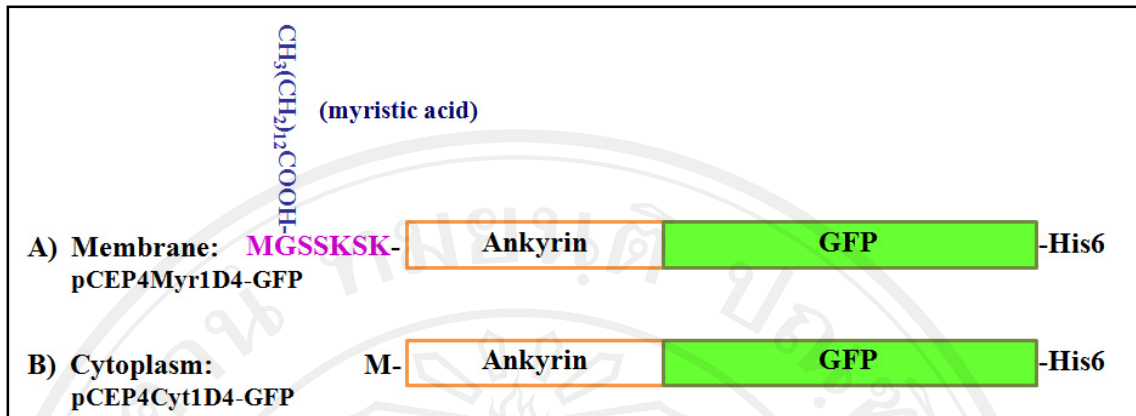


**Figure 3.21 Schematic representation of two constructed vectors for stable lines generation.** pCEP4-based vector was inserted with two different DNA fragment coding ankyrin binder (1D4), green fluorescence protein (GFP) and Histidine tag with myristoylation signal (**Membrane Myr<sup>+</sup>, A**) and without signal (**Cytoplasm, Myr<sup>-</sup>, B**) at N-terminus. Myristic acid covalently linked with glycine (G) is highlighted in blue letters.

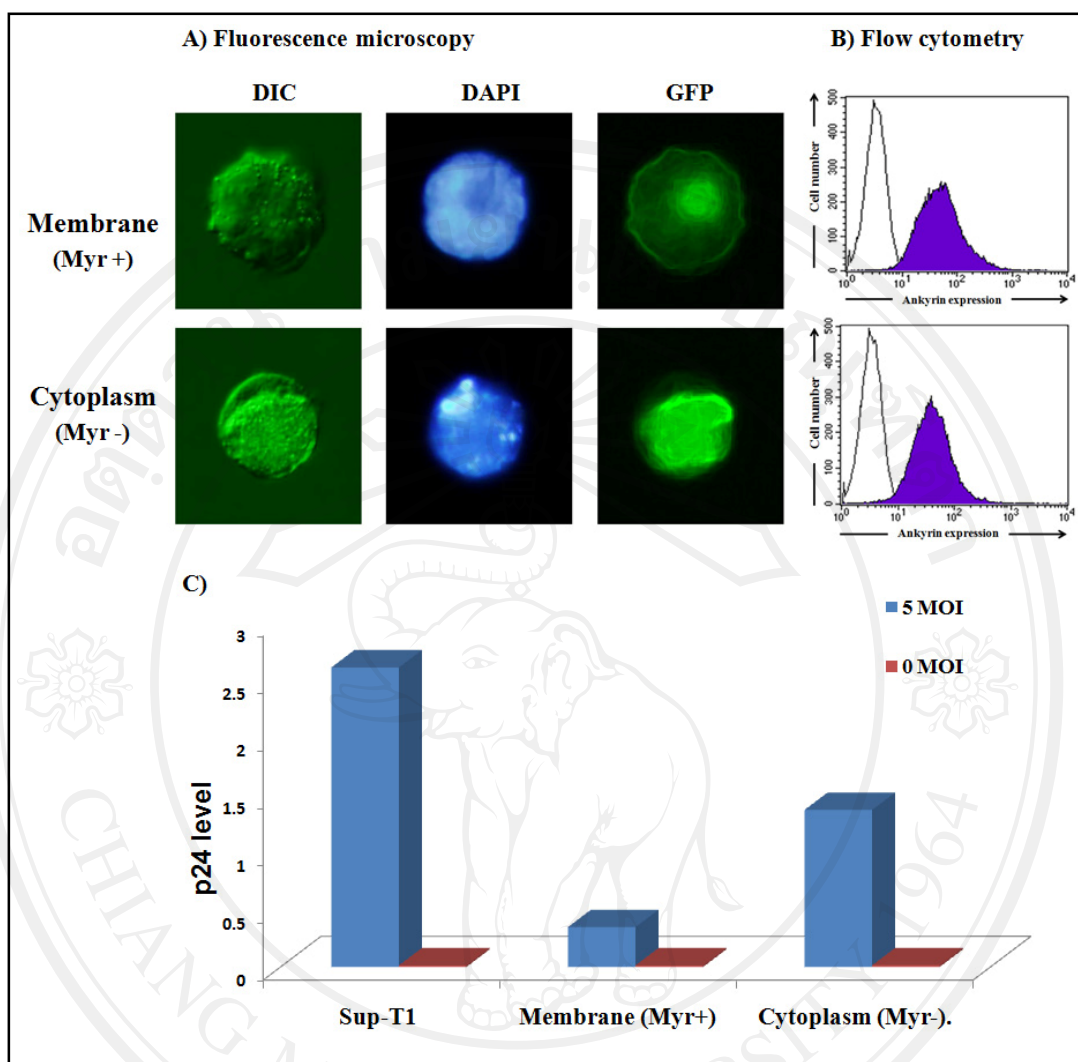


**Figure 3.22 Interference of HIV assembly by ankyrin binder 1D4 in different cellular compartments.** (A) Intracellular expression and localization of ankyrin binder 1D4 were observed under fluorescence microscopy. Cell shape, nucleus, and GFP-fused ankyrin protein were visualized by bright view (DIC), DAPI staining (DAPI), and green fluorescence channel (GFP), respectively. (B) Flow cytometry demonstrated the population of GFP positive cells. (C) The level of p24 measured from stable cell lines challenged with HIV<sub>NL4-3</sub>. Sup-T1 was used as control.